energies

MDPI

Article

Distributed Low-Carbon Energy Management of Urban Campus for Renewable Energy Consumption

Kan Yu [1,2,*], Qiang Wei [1,2], Chuanzi Xu [3], Xinyu Xiang [3] and Heyang Yu [4,*]

[1] Architectural Design and Research Institute of Zhejiang University Co., Ltd., Hangzhou 310028, China; weiq@zuadr.com
[2] Center for Balance Architecture, Zhejiang University, Hangzhou 310028, China
[3] Hangzhou Power Supply Company, State Grid Zhejiang Electric Power Co., Ltd., Hangzhou 310016, China; 389396733@qq.com (C.X.); myxiangxinyu@aliyun.com.cn (X.X.)
[4] College of Electrical Engineering, Zhejiang University, Hangzhou 310027, China
* Correspondence: edewfwe@foxmail.com (K.Y.); yuheyang@zju.edu.cn (H.Y.)

Abstract: In order to solve the mismatch between renewable energy and load in urban building microgrids, that is, the problem of renewable energy consumption in building microgrid clusters, while preserving the privacy of each user, this paper proposes a distributed low-carbon energy management method for urban building microgrid clusters. First, a low-carbon energy management method for the urban building microgrid is proposed in order to coordinate the power sharing of various subjects to minimize the total economic cost, unleash the consumption potential of low-carbon building clusters for renewable energy, and reduce carbon emissions on the spatial and time scale. Second, an ADMM-based distributed optimal energy management method is proposed to meet user energy needs while preserving local privacy; this includes energy storage systems, renewable energy generation, and the loads within each urban building microgrid. Finally, simulation experiments are conducted based on actual data from a certain area in Hangzhou, China, and the results verify the effectiveness of the model.

Keywords: alternating direction method of multipliers (ADMM); building microgrid; distributed optimization; low-carbon energy management; renewable energy consumption

Citation: Yu, K.; Wei, Q.; Xu, C.; Xiang, X.; Yu, H. Distributed Low-Carbon Energy Management of Urban Campus for Renewable Energy Consumption. *Energies* **2024**, *17*, 6182. https://doi.org/10.3390/en17236182

Academic Editor: Ahmed Abu-Siada

Received: 12 November 2024
Revised: 29 November 2024
Accepted: 4 December 2024
Published: 8 December 2024

1. Introduction

In the context of "carbon peak and carbon neutrality" objectives in China, the energy and power sector is pivotal in achieving substantial emission reductions. The establishment of building microgrids (MGs) [1], comprising renewable energy sources (RESs) [2], energy storage systems (ESSs), and various loads within urban distribution networks, can significantly enhance the consumption and control capabilities of renewable energy. As high-penetration renewable energy becomes increasingly integrated into urban distribution networks, the interconnection and cooperative operation of these microgrids will emerge as a crucial strategy for augmenting the capacity for renewable energy consumption. Simultaneously, the integration of high-penetration renewable energy into the distribution network is a key element in the low-carbon development of the power system.

At present, the carbon trading market is in a comprehensive development stage, and there have been many studies on low-carbon operation under the carbon trading mechanism [3,4]. X. Zhong et al. [5] propose an optimal energy management strategy for multi-energy microgrids considering carbon emissions, and develop a distributed algorithm to preserve the privacy of microgrids. L. Kong et al. [6] consider carbon benefits and propose a dual-layer energy low-carbon optimization scheduling method for electricity–hydrogen–thermal energy on campus based on the alternating direction of multipliers. H. Kong et al. [7] propose an optimal scheduling model of an integrated energy microgrid by considering multi-time-scale energy storage, and analyze the carbon

emissions for the analysis of the economic and environmental benefits of the microgrid. A. Mirzapour-Kamanaj et al. [8] develop a multi-follower bi-level optimization framework for the optimal interaction of energy hubs and the distribution network. W. Hua et al. [9] propose a novel blockchain-based peer-to-peer trading framework to trade energy and carbon allowance. P. Feng et al. [10] establish an optimization model that minimizes both energy costs and carbon emissions to evaluate environmental impact, aiming to create policies that save energy and reduce emissions. Y. Xiao et al. [11] proposes a optimization strategy for wind–solar–energy–storage microgrids with regard to green certificate trading and carbon emission constraints. However, the above research has not considered the issue of interconnection and the operation of urban-level building microgrids with a high rate of renewable energy usage in a low-carbon context to promote carbon emission reduction and renewable energy consumption.

Considering that in practical situations, urban building microgrids are managed by different entities, and each microgrid contains a large amount of private information such as user characteristics, load types, and power and energy storage configurations, it is necessary to construct a distributed economic dispatch model to coordinate the interconnected system. The urban-level building microgrid cluster is interconnected through the power network, and each building microgrid manages its own power source, load, and energy storage, providing only limited boundary information to the outside world. Therefore, distributed optimization methods [12,13] have more advantages than centralized optimization methods. The distributed control method is more in line with the interests of users than the traditional centralized method [14]. H. Yu and Z. Yuan et al. [15–17], respectively, adopt different distributed optimization algorithms. In [15], based on a mixed-integer model, a two-layer framework comprising a load aggregator and residents is developed to solve the model above, based on the alternating direction method of multipliers (ADMM). B. Zou [18] proposes an improved, distributionally robust, chance-constrained method to enhance the power flexibility of an Internet data center. In [16], the researchers propose a probabilistic distributed control method to help users formulate the electric vehicle charging plan independently. S. Mhanna et al. [19] propose a double smoothing dual function to solve the distributed and parallel problem of the non-convex demand response. M. Latifi et al. [20] propose a diffusion–ADMM strategy to balance the goals of customers and the distribution system operator (DSO). It can be seen that ADMM supports distributed computing and has scalability. However, privacy-preserving distributed optimization techniques for the integration of urban-level building microgrids for low-carbon operations have not been considered in past research.

In order to overcome the two technical difficulties identified above, this paper proposes a distributed low-carbon energy management method for urban building microgrid clusters. Considering the complexity of the system structure, a layered optimization scheme is adopted. The upper level aims to coordinate the power sharing of various building microgrids, maximize the collaborative consumption of renewable energy, minimize the total economic cost, and unleash the consumption potential of low-carbon building clusters for renewable energy. The lower-level model coordinates and controls the energy storage systems, renewable energy generation, and loads within each urban building microgrid, establishes a low-carbon dispatch model for urban buildings, meets user energy needs, aims to improve the economic efficiency of system operation, reduces system carbon emissions, and enhances the consumption capacity of renewable energy.

The main contributions of this article are summarized as follows:

(1) The low-carbon energy management of an urban building microgrid is proposed in order to coordinate the power sharing of various subjects to enhance renewable energy consumption and reduce carbon emissions on the spatial and time scale.
(2) An ADMM-based distributed optimal energy management method is proposed to preserve local privacy, such as in energy storage systems, renewable energy generation, and the loads within each urban building microgrid.

The remainder of this paper is arranged as follows. Section 2 defines the problem to be solved and visualizes it in an illustrative framework. Section 3 formulates the mathematical model, including a power and carbon emissions model for urban campus energy usage, and the objective function and constraints. Section 4 provides a privacy-preserving distributed algorithm. Section 5 offers the analysis and results of the numerical experiments. Finally, the conclusions are summarized in Section 6.

2. Problem and System Framework

The microgrid system framework considered in this article mainly includes wind turbines, photovoltaic (PV) power generation systems, micro gas turbines, energy storage systems, and loads, as shown in Figure 1. The system regulates the output of traditional power generation resources, renewable energy resources, and energy storage systems under the microgrid through a unified energy management platform, with the goal of minimizing the system's economic and carbon emission costs. While ensuring low costs, the system coordinates the output of renewable energy to regulate the system.

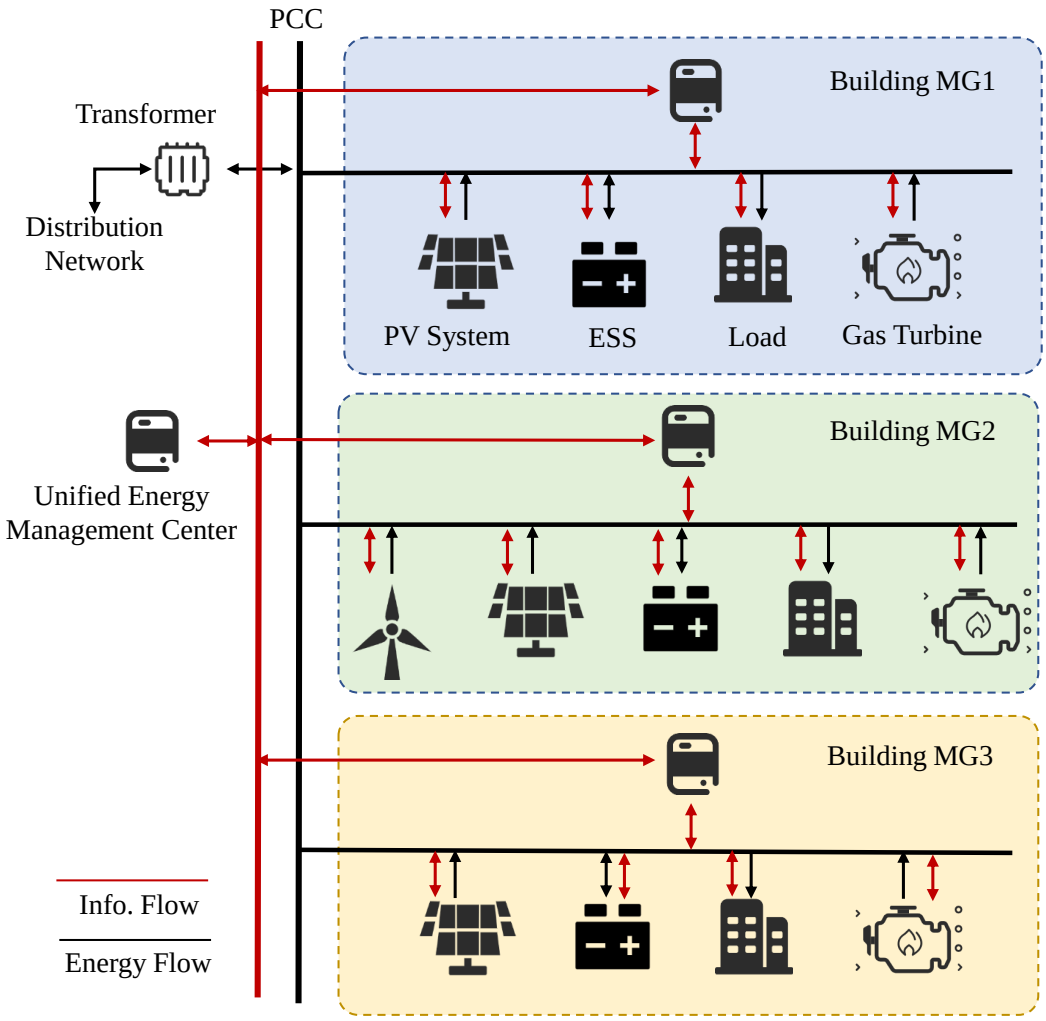

Figure 1. Diagram of building microgrid cluster structure.

3. Mathematical Model

3.1. Cost Model for Urban Building Microgrid Energy Usage

3.1.1. Gas Turbine

The operating cost of a gas turbine consists of the fuel cost $C_{i,t}^{gas}$ (1) and carbon emission cost $C_{i,t}^{gas,CO_2}$ (2), which can be expressed as follows:

$$C_{i,t}^{gas} = b_i^{gas} P_{i,t}^{gas} \delta t \quad (1)$$

$$C_{i,t}^{gas,CO_2} = \rho_t^{CO_2} e_{i,t}^{gas,CO_2} P_{i,t}^{gas} \delta t \quad (2)$$

where b_i^{gas} is the cost coefficient of the i-th gas turbine; $P_{i,t}^{gas}$ is the output power of the i-th gas turbine at the t-th period; $\rho_t^{CO_2}$ is the price of CO_2 at the t-th period; and $e_{i,t}^{gas,CO_2}$ is the dynamic carbon emission factor (CEF) of the i-th gas turbine at the t-th period. We suppose that all required scheduling periods in a day are finite and divided into T equal sub-intervals. We define $\boldsymbol{T}$ as the set indices of all equal sub-intervals, that is, $t \in \boldsymbol{T} : \{1, 2, ..., T\}$.

3.1.2. Renewable Energy Resources

The renewable energy resources mainly considered in this research include photovoltaic power generation systems and wind turbines. It is emphasized here that, without considering the installation costs of PV systems and wind turbines, this research assumes that the operating and maintenance costs of PV systems $C_{i,t}^{PV}$ and wind turbines $C_{i,t}^{wind}$ are very small, and that their carbon emissions are 0.

$$C_{i,t}^{PV} = b_i^{PV} P_{i,t}^{PV} \delta t \quad (3)$$

$$C_{i,t}^{wind} = b_i^{wind} P_{i,t}^{wind} \delta t \quad (4)$$

$$C_{i,t}^{PV,CO_2}, C_{i,t}^{wind,CO_2} = 0 \quad (5)$$

where b_i^{PV} and b_i^{wind} are, respectively, the operating and maintenance cost coefficients of the i-th PV system and i-th wind turbine; $C_{i,t}^{PV,CO_2}$ and $C_{i,t}^{wind,CO_2}$ are, respectively, the carbon emission cost of the i-th PV system and i-th wind turbine at the t-th period; and $P_{i,t}^{PV}$ and $P_{i,t}^{wind}$ are, respectively, the output power of the i-th PV system and i-th wind turbine at the t-th period.

3.1.3. Energy Storage System

In order to smooth out the fluctuations in the output of renewable energy generation and improve th renewable energy generation absorption rate, urban building microgrids are often equipped with ESSs with a certain capacity. The operating cost of the energy storage system mainly considers the charging and discharging costs during the operation process, while the carbon emission cost is mainly determined by the carbon emission factor of the common coupling point (PCC) between the building microgrids and public bus during charging and discharging. The operating costs of the ESS $C_{i,t}^{ess}$ and the carbon emission cost $C_{i,t}^{ess,CO_2}$ can be expressed as follows:

$$C_{i,t}^{ess} = c_i^{ess} \left(\frac{P_{i,t}^{ess,d}}{\eta_i^d} + P_{i,t}^{ess,c} \eta_i^c \right) \delta t \quad (6)$$

$$C_{i,t}^{ess,CO_2} = \rho_t^{CO_2} e_{i,t}^{pcc,CO_2} P_{i,t}^{ess,c} \delta t \quad (7)$$

where c_i^{ess} is the charge and discharge cost coefficient of i-th ESS; $P_{i,t}^{ess,c}$ and $P_{i,t}^{ess,d}$ are, respectively, the charge and discharge power of i-th ESS at the t-th period; η_i^c and η_i^d are, respectively, the charge and discharge efficiency of i-th ESS; and $e_{i,t}^{pcc,CO_2}$ is the dynamic carbon emission factor of the PCC of i-th ESS at the t-th period.

3.1.4. Purchasing of Electricity

Each building in the urban building microgrid group can meet the demand for power during a shortage by purchasing electricity. In this work, we assume that the main grid does not accept electricity sales from building microgrids. Hence, the purchasing electricity cost $C_{i,t}^{grid}$ (8) and carbon emission cost of the buildings $C_{i,t}^{grid,CO_2}$ (9) can be shown as follows:

$$C_{i,t}^{grid} = c_{i,t}^{grid,b} P_{i,t}^{grid,b} \delta t \tag{8}$$

$$C_{i,t}^{grid,CO_2} = \rho_t^{CO_2} e_{i,t}^{pcc,CO_2} P_{i,t}^{grid,b} \delta t \tag{9}$$

$$P_{i,t}^{grid,b} \geq 0 \tag{10}$$

where $c_{i,t}^{grid,b}$ is, respectively, the electricity purchase price between the building microgrid and the main grid at the t-th period; and $P_{i,t}^{grid,b}$ is the purchasing power between the building microgrid and the main grid at the t-th period.

3.2. Objective Function

This research takes a building microgrid as the research object, comprehensively considering the overall economic operation of the microgrid and the promotion of carbon emission reduction. The objective function of the model built is set to minimize the overall cost of the microgrid, including the operating costs of various devices in the microgrid, the cost of purchasing electricity in the microgrid, and the cost of carbon emissions, as shown below:

$$\begin{aligned} \min C^{total} =& C^{cost} + C^{CO_2} \\ =& \sum_{t=1}^{T} (\sum_{i=1}^{N_g} C_{i,t}^{gas} + \sum_{i=1}^{N_p} C_{i,t}^{PV} + \sum_{i=1}^{N_w} C_{i,t}^{wind} + \sum_{i=1}^{N_e} C_{i,t}^{ess} + C_{i,t}^{grid}) \\ &+ \sum_{t=1}^{T} (\sum_{i=1}^{N_g} C_{i,t}^{gas,CO_2} + C_{i,t}^{grid,CO_2}) \end{aligned} \tag{11}$$

where C^{total} is the total cost of the building microgrid; C^{cost} and C^{CO_2} are, respectively the total power generation cost and total carbon emission cost of the building microgrid components; and N_g, N_p, N_w, N_e are, respectively the total number of gas turbines, PV systems, wind generation systems and ESSs.

3.3. Constraints

3.3.1. Gas Turbine

The operational constraints of gas turbines comprise upper and lower-limit constraints for the output power (12) and the power ramp constraints (13) and (14), which are shown as follows:

$$P_i^{gas,min} \leq P_{i,t}^{gas} \leq P_i^{gas,max} \tag{12}$$

$$0 \leq P_{i,t}^{gas} - P_{i,t-1}^{gas} \leq P_i^{gas,up,max} \tag{13}$$

$$0 \leq P_{i,t-1}^{gas} - P_{i,t}^{gas} \leq P_i^{gas,down,max} \tag{14}$$

where $P_i^{gas,min}$ and $P_i^{gas,max}$ are, respectively, the upper and lower limit of the active output power of the i-th gas turbine; and $P_i^{gas,up,max}$ and $P_i^{gas,down,max}$ are, respectively, the maximum up ramp power and down ramp power of the i-th gas turbine.

3.3.2. PV Systems

Considering the different characteristics of PV power generation output, different upper limits are set to constrain the PV output. Meanwhile, this research does not consider the uncertainty of PV output and its reactive power output. The operational constraints of PV are shown as (15):

$$0 \leq P_{i,t}^{PV} \leq P_i^{PV,max} \tag{15}$$

where $P_i^{PV,max}$ is the maximum output active power of the i-th PV power generation unit of building i.

3.3.3. Wind Generation System

Similar to the output characteristics of PV power generation systems, we set different upper limits for wind generation systems in order to constrain their output. Meanwhile, this work did not take into account its uncertainty. The operational constraints of the wind generation system are shown in (16):

$$0 \le P_{i,t}^{wind} \le P_i^{wind,max} \tag{16}$$

where $P_i^{wind,max}$ is the maximum output active power of the i-th wind power generation unit of building i.

3.3.4. Energy Storage System

During the charging and discharging process, relevant restrictions need to be imposed on the charging and discharging status and power, using the following constraints:

$$0 \le P_{i,t}^{ess,c} \le u_{i,t}^{c} P_{i,t}^{ess,c,max} \tag{17}$$

$$0 \le P_{i,t}^{ess,d} \le u_{i,t}^{d} P_{i,t}^{ess,d,max} \tag{18}$$

$$u_{i,t}^{c} + u_{i,t}^{d} \le 1, u_{i,t}^{c}, u_{i,t}^{d} \in \boldsymbol{N} \tag{19}$$

$$s_i^{min} \le s_{i,t} \le s_i^{max} \tag{20}$$

$$s_{i,t} = s_{i,t-1} + \frac{u_{i,t}^{c} P_{i,t}^{ess,c} \eta_i^{c} \delta t}{e_i^{ess}} - \frac{u_{i,t}^{d} P_{i,t}^{ess,d} \delta t}{\eta_i^{d} e_i^{ess}} \tag{21}$$

$$s_{i,1} = s_{i,T} \tag{22}$$

where $u_{i,t}^{c}$ and $u_{i,t}^{d}$ are, respectively, the charge and discharge state variable of i-th ESS at the t-th period, and where both are not equal to 1 at the same time; $\boldsymbol{N}$ is the set of natural numbers; and $s_{i,t}$ is the state of charge (SOC) of i-th ESS at the t-th period. Meanwhile, s_i^{min} and s_i^{max} are, respectively, the specified minimum and maximum SOC of i-th ESS. Equation (19) ensures that the ESS can have three states at the same time, which are, respectively, charging, discharging, and standby. Equation (22) guarantees that the ESS can restore its initial state during daily operation.

3.3.5. Power Balance Constraint

The whole microgrid system needs to ensure power balance at each time period, using the following constraints:

$$P_t^{load} = \sum_{i=1}^{N_g} P_{i,t}^{gas} + \sum_{i=1}^{N_p} P_{i,t}^{PV} + \sum_{i=1}^{N_w} P_{i,t}^{Wind} + P_t^{grid} + \sum_{i=1}^{N_e} P_t^{ess} \tag{23}$$

where P_t^{load} is the total power of the load at the t-th period.

4. Distributed Optimization

4.1. Basic Principle

The unified energy management model proposed in the previous section is a mixed-integer quadratic linear programming problem, which requires building microgrids to transfer the configuration information, control rights, and load information of the power generation resources they manage to a unified energy management operator, resulting in serious privacy leakage issues. In addition, due to the high demand for computing resources, binary variables, and a slower convergence speed when the number of participants increases, we introduce ADMM to decompose the traditional unified energy management model. This method can enable the collaborative consumption of renewable energy between building microgrids and unified operators without exchanging sensitive information, while only requiring the total power of the interaction gateway; this fundamentally protects the privacy of each building microgrid. In addition, ADMM can be regarded as a combination of dual decomposition and augmented Lagrangian multiplier

methods, ensuring good decomposability, convergence, and a fast computational speed, thus possessing excellent scalability.

The general ADMM equation can be modeled as follows:

$$\min \quad f(\boldsymbol{x}) + g(\boldsymbol{y}) \tag{24}$$

$$\text{s.t.} \quad A\boldsymbol{x} + B\boldsymbol{y} = C \tag{25}$$

where $\boldsymbol{x}$ and $\boldsymbol{y}$ are two sets of separable variables, and $f(\boldsymbol{x})$ and $g(\boldsymbol{y})$ are two sets of separable objective functions. Meanwhile, Equation (25) shows the coupling relationship between two sets of variables. The augmented Lagrangian form of ADMM can be represented as follows:

$$\begin{aligned} L_{\rho_1}(\boldsymbol{x}, \boldsymbol{y}, \boldsymbol{\lambda}) =& f(\boldsymbol{x}) + g(\boldsymbol{y}) + \boldsymbol{\lambda}^T(A\boldsymbol{x} + B\boldsymbol{y} - C) \\ &+ \frac{\rho_1}{2} \cdot \|A\boldsymbol{x} + B\boldsymbol{y} - C\|_2^2 \end{aligned} \tag{26}$$

where $\boldsymbol{\lambda}$ is a dual variable, and ρ_1 is a penalty parameter of the augmented Lagrangian multiplier. Actually, there is no fixed standard for the determination of the penalty parameter. Therefore, we may set the value of ρ_1 as 2 or more.

Moreover, the primary and secondary residuals of ADMM in the k-th iteration are defined as follows:

$$\begin{cases} J^{(k)} = A\boldsymbol{x}^{(k)} + B\boldsymbol{y}^{(k)} - C \\ R^{(k)} = \rho_1 A^T B(\boldsymbol{x}^{(k)} - \boldsymbol{x}^{(k-1)}) \end{cases} \tag{27}$$

To decompose the objectives, within each iteration, Equation (26) is minimized over $\boldsymbol{x}$ with $\boldsymbol{y}$, which is obtained in the last iteration. Therefore, the equations for updating the values of $\boldsymbol{x}$, $\boldsymbol{y}$ and $\boldsymbol{\lambda}$ are shown in the following (28):

$$\begin{cases} \boldsymbol{x}^{(k)} = \arg\min\limits_{\boldsymbol{x}} L_{\rho_1}(\boldsymbol{x}, \boldsymbol{y}^{(k-1)}, \boldsymbol{\lambda}^{(k-1)}) \\ \boldsymbol{y}^{(k)} = \arg\min\limits_{\boldsymbol{y}} L_{\rho_1}(\boldsymbol{x}^{(k)}, \boldsymbol{y}, \boldsymbol{\lambda}^{(k-1)}) \\ \boldsymbol{\lambda}^{(k)} = \boldsymbol{\lambda}^{(k-1)} + \rho_1(A\boldsymbol{x}^{(k)} + B\boldsymbol{y}^{(k)} - C) \end{cases} \tag{28}$$

The iteration will stop when both $J^{(k)}$ and $R^{(k)}$, respectively, need to reach the primary and dual criteria, and when the iteration termination conditions fulfil the following formulas:

$$\begin{cases} \|J^{(k)}\|_2 \leq \epsilon^{\text{pri}} \\ \|R^{(k)}\|_2 \leq \epsilon^{\text{dual}} \end{cases} \tag{29}$$

where values of $\epsilon^{\text{pri}} > 0$ and $\epsilon^{\text{pri}} > 0$.

4.2. Information Exchange Process

The information exchange process of the distributed solving algorithm is shown in the figure. Distributed solving algorithms decompose a large problem into several subproblems that can be solved separately. The cluster's unified operator and each building microgrid only need to solve their own sub-optimization problems, and each subject only shares variables and auxiliary variables. The power information, energy storage power information, and load information within each building microgrid are only used for solving sub-problems on their own and are not shared with the public, fully protecting the privacy of all parties involved. The entire optimization problem can be simplified into two iterative processes: solving sub-problems and exchanging shared variables, which do not contain private information. In addition, the algorithm is highly scalable. Even if the number of microgrids further increases, the difficulty of solving each sub-problem will not change, and new entities can be easily added to the entire iteration process.

5. Case Study and Analysis

5.1. Parameter Setup

To verify the availability of the algorithm in this work, we consider a microgrid cluster consisting of three building microgrids. The scheduling interval is set to 1 h. In the case study of this work, the operating parameters of every component include the basic parameters of gas turbines and energy storage systems. The operating parameters of each microgrid component are shown in Table 1. In addition, the upper and lower limits of the PV and wind power output are determined based on typical output curves, and the expected load of each building microgrid is determined based on typical load curves, which are shown as Figure 2. The cost parameters of each microgrid component and carbon emission parameters are, respectively, shown in Tables 2 and 3. The carbon emission factor of the gas turbine and grid can be seen in Figure 3.

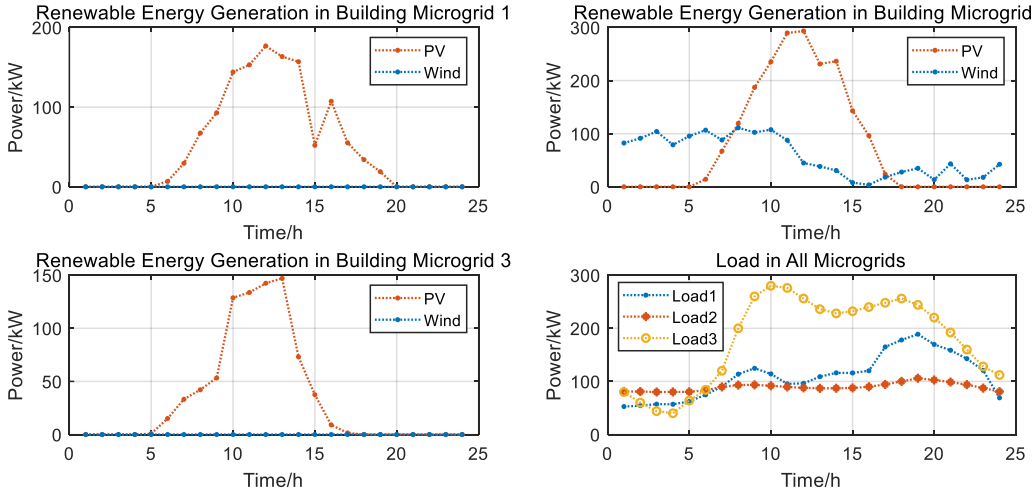

Figure 2. Typical PV, wind power and load curves of all building microgrids.

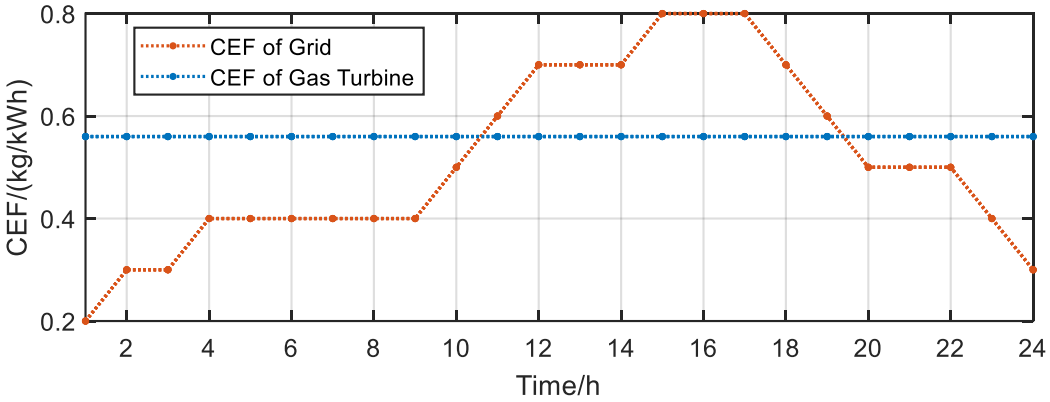

Figure 3. Carbon emission factor of gas turbines and grid.

Table 1. Component operating parameters of microgrid.

Parameters	Value	Parameters	Value
$P^{gas,max}$/kW	120	e^{ess}/kW·h	100
$P^{gas,min}$/kW	30	η^{c}	0.95
$P^{gas,up,max}$/kW	30	η^{d}	0.95
$P^{gas,down,max}$/kW	30	s^{max}	0.9
$P^{ess,c,max}$/kW	100	s^{min}	0.2
$P^{ess,d,max}$/kW	100	Charge and Discharge Rate	1 C

Table 2. Component cost parameters of microgrid.

Parameters	Value	Parameters	Value
b^{gas}/(CNY/kW·h)	0.70	b^{Wind}/(CNY/kW·h)	0.06
b^{PV}/(CNY/kW·h)	0.05	c^{ess}/(CNY/kW·h)	0.10

Table 3. Carbon emission parameters of microgrid.

Parameters	Value
ρ^{gas,CO_2}/(CNY/kg)	1.00
e^{gas,CO_2}/(kg/kW·h)	0.70
e^{pcc,CO_2}/(kg/kW·h)	Figure 3

The purchase price of electricity from the microgrid to the grid is taken from the typical peak and valley electricity prices of industrial and commercial users in Zhejiang Province, as shown in Table 4.

Table 4. Typical electricity price of industrial and commercial users in Hangzhou, China [15].

Type	Time (h)	Price (CNY)
Peak Period	8:00–11:00, 13:00–17:00	1.05
Regular Period	17:00–24:00	0.67
Valley Period	0:00–8:00, 11:00–13:00	0.32

In Figure 2, it can be seen that the only renewable energy resource of building microgrids 1 and 3 is PV, while the renewable energy resources of building microgrid 2 contain wind power and PV. Meanwhile, we can see that building microgrid 2 has abundant renewable energy resources, with the highest predictive output, while building microgrid 3 has the lowest predictive power generation. It can also be seen that among these three building microgrids, building microgrid 3 has the heaviest load, while building microgrid 2 has the lightest load. Therefore, the overall situation of surplus renewable energy in building microgrid 2 and insufficient renewable energy in building microgrid 3 reflects the potential for the complementary adjustment of building microgrid clusters.

The numerical simulation is mainly carried out on a computer equipped with 16 Intel Intel i5-13500H 2.60 GHz CPU and 32 GB RAM. The main problem and sub-problems are solved by a CBC solver. Matlab is used for modeling and implementation.

5.2. Comparison of Different Scenarios

In order to test the effectiveness of the proposed algorithm scheme, three different control scenarios were set up in this section to verify the effectiveness of the algorithm. Here, the renewable energy consumption rate is defined as CR^{RES}, as shown in (30).

$$CR^{RES} = \frac{\sum_{t=1}^{T}(\sum_{i=1}^{N_p} P_{i,t}^{PV,r} + \sum_{i=1}^{N_w} P_{i,t}^{wind,r})}{\sum_{t=1}^{T}(\sum_{i=1}^{N_p} P_{i,t}^{PV,f} + \sum_{i=1}^{N_w} P_{i,t}^{wind,f})} \tag{30}$$

where $P_{i,t}^{PV,r}$ and $P_{i,t}^{wind,r}$ are, respectively, the real output power of the i-th PV system and i-th wind turbine at the t-th period; and $P_{i,t}^{PV,f}$ and $P_{i,t}^{wind,f}$ are, respectively, the predictive value of the output power of the i-th PV system and i-th wind turbine at the t-th period.

5.2.1. Scenario Setup

Case 1: Without considering of electricity sharing among microgrids;

Case 2: Considering electricity sharing among microgrids but without considering user's privacy;

Case 3: Considering electricity sharing among microgrids and user's privacy.

In this section, we first consider whether to implement unified energy management or autonomous energy management for each building microgrid. In unified energy management, each building microgrid is connected to the same power distribution bus and interacts with the main grid through a unified power port. At the same time, mutual power benefits can be achieved among microgrids. When building microgrids engage in autonomous energy management, there is no mutual power benefit among them. Therefore, **Case 1** and **Case 2** are used to verify the superiority of unified energy management. When users focus on preserving their privacy information, such as internal component configurations, power generation and load data, and are unwilling to disclose them, **Case 2** and **Case 3** will be used to test the effectiveness of distributed algorithms.

5.2.2. Comparison of Different Energy Management Method

In **Case 1**, the proposed autonomous energy management strategy is only used to consider operation and maintenance costs. Based on the optimal objective function of total costs (fuel, operation and maintenance costs, carbon emission costs), the system will prioritize the use of renewable energy generation to meet load demand, and the excess renewable energy electricity will be used to charge the energy storage system until it reaches its maximum capacity. The additional electricity in the energy storage system will be used to supply power with priority to the system load when the electricity prices and carbon emission factors are at their peak, while renewable energy generation resources are scarce. When both the energy storage system and renewable energy generation are insufficient, the system will choose between local gas turbine power generation or purchasing electricity from the main grid based on cost factors. In **Case 2**, the unified energy management strategy proposed is not significantly different from the autonomous energy management strategy outlined in Case 1. The main difference is that in the unified energy management strategy, the system can coordinate all resources of all building microgrid users, including gas turbines, renewable energy resources, energy storage systems, etc.

It can be observed in Figures 2, 4 and 5 that in **Case 1**, building microgrid 2 is equipped with abundant renewable energy resources, including small wind turbines and solar power generation resources with a peak power of about 300 kW. However, its load level is quite low, and the periods of high renewable energy generation are mismatched with the peak load periods, resulting in the significant waste of renewable energy resources. On the contrary, the load level in building microgrid 3 is quite high, while the level of renewable energy it is equipped with is relatively low. For most of the time, renewable energy resources are insufficient to ensure power supply, so local gas turbines or the purchase of electricity from the main grid are needed to achieve sufficient power supply. In **Case 2**, under the unified energy management strategy, the renewable energy resources of building microgrids 1, 2, and 3 can be mutually beneficial, and the overall proportion of renewable energy consumption can be further increased to jointly meet the common load demand of building microgrids 1, 2, and 3, achieve the maximization of renewable energy utilization, and reduce the cost of power generation and carbon emissions.

Table 5 shows a comparison of the various economic costs, carbon emission costs of each building microgrid, and total costs under unified energy management and autonomous energy management. It can also be clearly seen from Table 5 that the unified management of microgrids in various buildings can achieve a significant reduction in total costs while further improving the overall renewable energy consumption rate. In particular, the total economic cost and carbon emission cost of purchasing electricity from the main e-commerce platform have decreased even more. The reason for this can be summarized as follows: unified energy management eliminates the mismatch between the supply and demand of renewable energy and load in certain sub-microgrids (supply–demand regulation on the spatial scale), enables the mutual utilization of renewable energy resources between different building microgrids, improves the utilization rate of renewable energy, and reduces the cost of purchasing electricity and carbon emissions.

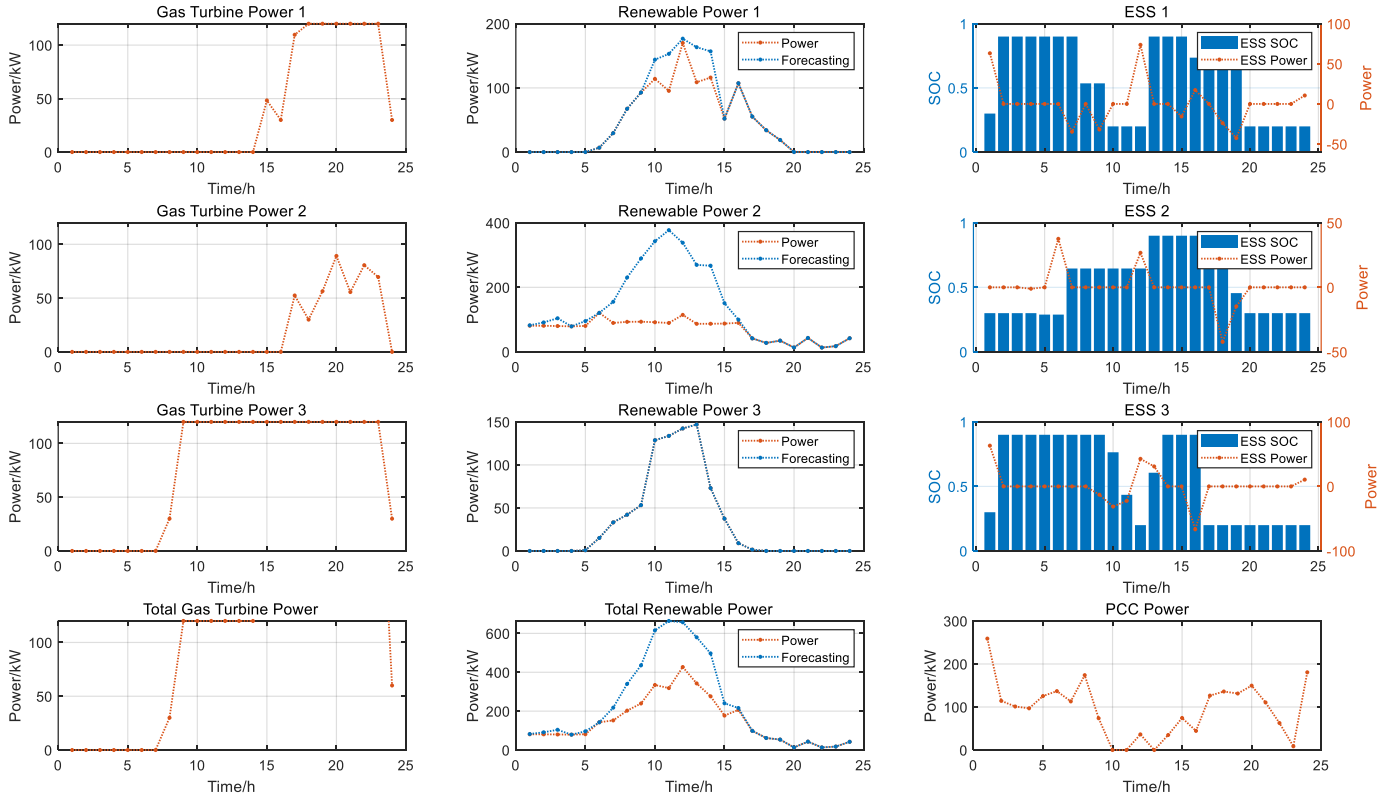

Figure 4. Power curves of various components in each building microgrid for autonomous energy management (**Case 1**).

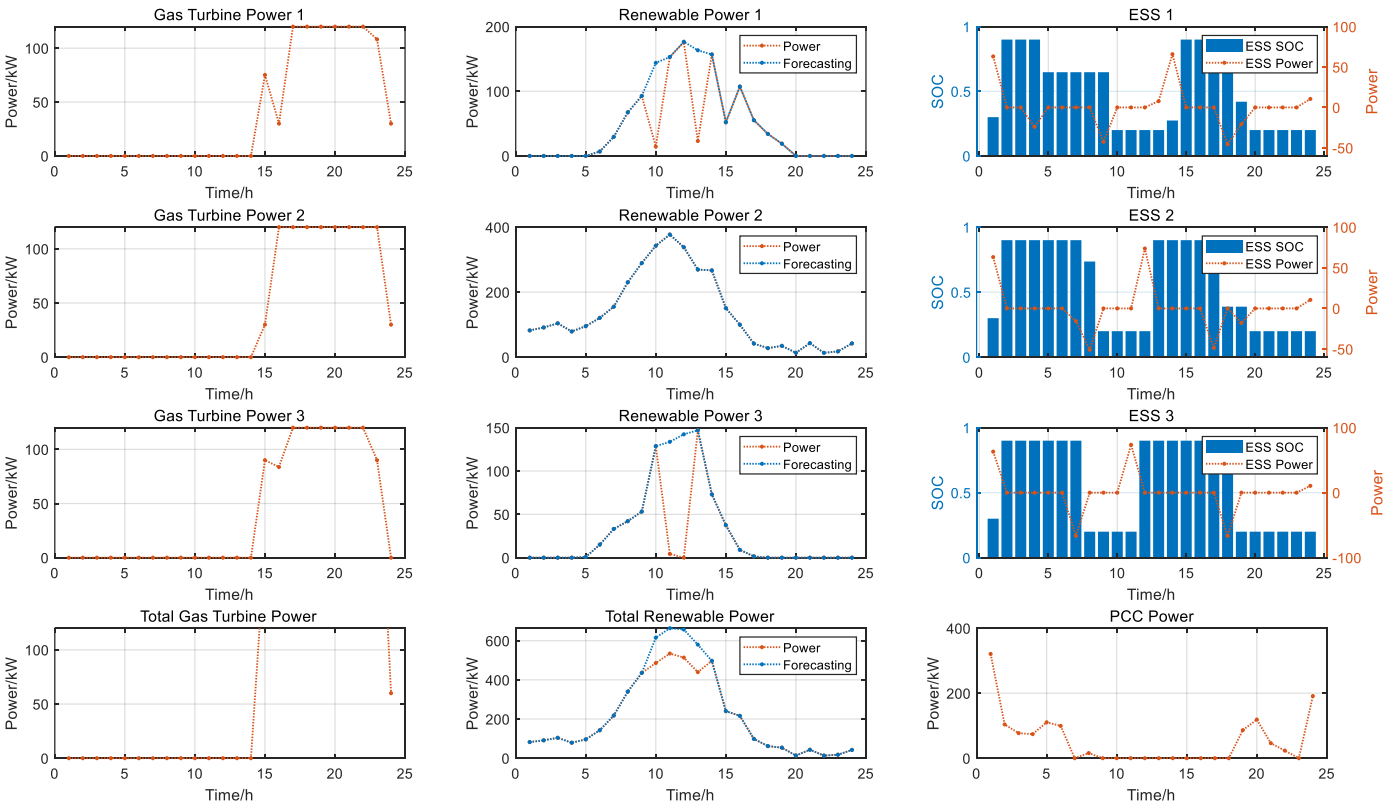

Figure 5. Power curves of various components in each building microgrid for unified energy management (**Case 2**).

Table 5. The results of operating and carbon emission costs for each building microgrid and all building microgrids.

Case 1				
Type	**Total**	**Building MG 1**	**Building MG 2**	**Building MG 3**
C^{total}	5718.66	1495.53	555.25	3667.88
C^{gas}	2262.27	656.55	303.72	1302.00
C^{grid}	1264.58	268.72	25.78	970.08
C^{gas,CO_2}	969.54	281.38	130.16	558.00
C^{grid,CO_2}	1043.94	235.45	11.55	796.94
CR^{RES}	66.00%	84.93%	50.49%	100.00%
Case 2				
Type	**Total**	**Building MG 1**	**Building MG 2**	**Building MG 3**
C^{total}	4220.44	∼	∼	∼
C^{gas}	2076.98	674.40	714.00	688.58
C^{grid}	568.60	∼	∼	∼
C^{gas,CO_2}	890.13	289.03	306.00	295.10
C^{grid,CO_2}	441.66	∼	∼	∼
CR^{RES}	89.96%	78.47%	100.00%	66.76%

5.2.3. Effectiveness of Distributed Methods

To verify the effectiveness of the distributed algorithm, the value of ρ_1 is 2, and the iteration of the distributed algorithm is shown in the Figure 6. From Figure 6, it can be seen that the primary residual continuously decreases during the iteration process and converges when the number of iterations is 10. Correspondingly, the target value in Figure 6 also reaches its optimum when the number of iterations is 10. It can be seen from Figure 6 that there is basically no difference in the results between distributed algorithms and centralized algorithms, which meet the requirements of practical applications. Distributed algorithms converge quickly and meet practical requirements.

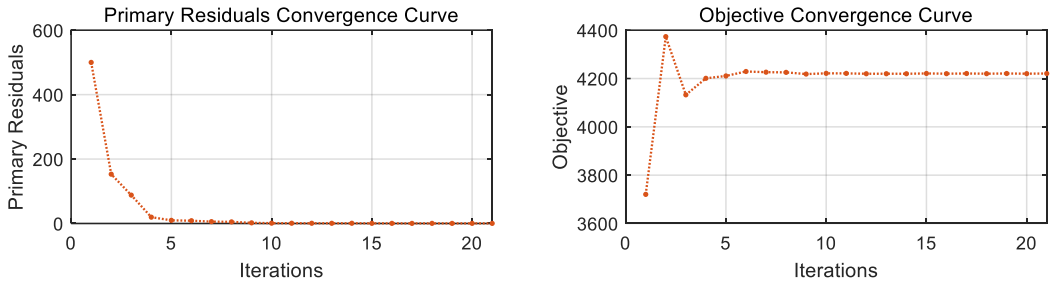

Figure 6. Iterative process of the algorithm (**Case 3**).

5.3. The Impact of ESS Parameters

In this section, we mainly study the effects of the capacity of ESSs in building microgrid systems on system economic costs, carbon emission costs, and renewable energy consumption rates, in order to provide reasonable references for configuring ESSs in building microgrid systems. In this section, this case has considered electricity sharing among microgrids and user's privacy.

Table 6 shows the total economic cost, total carbon emission cost, and total renewable energy consumption rate when the microgrid of each building is equipped with ESSs with different capacities. Here, we set the charging and discharging rate of the ESS to 1 C. It can be observed from Table 6 that, as the capacity of the ESS in the building microgrid increases, both economic and carbon emission costs decrease, while the total renewable

energy consumption rate significantly increases. The reason for this is that when the capacity provided by the ESS increases, during periods of high renewable energy resource supply and insufficient load demand, the system can further store excess renewable energy resources to meet the load demand when renewable energy is scarce and the cost of purchasing electricity is high, achieving supply–demand regulation in building microgrid systems on the time scale.

Table 6. Various costs and total renewable energy consumption rate for each building and ESSs equipped with different capacities.

Parameter	**Results**			
Capacity of ESS	**100**	**200**	**300**	**400**
C^{total}	4220.44	3974.96	3761.65	3637.69
C^{gas}	2076.98	2076.98	2001.21	1888.14
C^{grid}	568.60	452.89	403.51	428.44
C^{gas,CO_2}	890.13	890.13	857.66	809.20
C^{grid,CO_2}	441.66	300.84	234.10	241.70
CR^{RES}	89.96%	94.05%	98.14%	100.00%

6. Conclusions

This paper proposes a distributed low-carbon energy management method for urban building microgrid clusters. First, a low-carbon energy management method for urban building microgrids is proposed in order to coordinate the power sharing of various subjects to minimize the total economic cost, reveal the consumption potential of low-carbon building clusters for renewable energy, and reduce carbon emissions on the spatial and time scale. Second, an ADMM-based distributed optimal energy management method is proposed to meet the needs of users while preserving local privacy, such as information about the energy storage systems, renewable energy generation, and the loads within each urban building microgrid. In the future, further consideration needs to be given to the mechanisms associated with transaction modes and transaction prices in microgrids for the distributed low-carbon energy management of urban power.

Author Contributions: Writing—original draft preparation, K.Y. and Q.W.; writing—review and editing, H.Y.; visualization, H.Y.; supervision, C.X. and X.X.; project administration, C.X. and X.X. All authors have read and agreed to the published version of the manuscript.

Funding: This research was funded in part by the Key R&D Program of Zhejiang Province (No. 2024C03247) and in part by the Research Project of Center for Balance Architecture, Zhejiang University (No. 2020-RD49).

Data Availability Statement: The datasets presented in this article are not readily available because of confidentiality restrictions.

Conflicts of Interest: Authors Kan Yu and Qiang Wei were employed by the company Architectural Design and Research Institute of Zhejiang University Co., Ltd. Author Xinyu Xiang was employed by the company Hangzhou Power Supply Company, State Grid Zhejiang Electric Power Co., Ltd. The remaining authors declare that the research was conducted in the absence of any commercial or financial relationships that could be construed as a potential conflict of interest.

Abbreviations

The following abbreviations are used in this manuscript:

ADMM	Alternating Direction Method of Multipliers
CBC	Coin or Branch and Cut
CEF	Carbon Emission Factor
CPU	Central Processing Unit

DSO	Distribution System Operator
ESS	Energy Storage System
MG	Microgrid
PCC	Point of Common Coupling
PV	Photovoltaic
RAM	Random Access Memory
RES	Renewable Energy Source
SOC	State of Charge

References

1. Solanki, B.V.; Raghurajan, A.; Bhattacharya, K.; Cañizares, C. Including Smart Loads for Optimal Demand Response in Integrated Energy Management Systems for Isolated Microgrids. *IEEE Trans. Smart Grid* **2015**, *8*, 1739–1748. [CrossRef]
2. Zuo, K.; Sun, M.; Zhang, Z.; Cheng, P.; Strbac, G.; Kang, C. Transferability-Oriented Adversarial Robust Security-Constrained Optimal Power Flow. *IEEE Trans. Smart Grid* **2024**, *15*, 5169–5181. [CrossRef]
3. Chen, L.; Gao, L.; Xing, S.; Chen, Z.; Wang, W. Zero-carbon microgrid: Real-world cases, trends, challenges, and future research prospects. *Renew. Sustain. Energy Rev.* **2024**, *203*, 114720. [CrossRef]
4. Mu, C.; Ding, T.; Zhu, S.; Han, O.; Du, P.; Li, F.; Siano, P. A Decentralized Market Model for a Microgrid with Carbon Emission Rights. *IEEE Trans. Smart Grid* **2022**, *14*, 1388–1402. [CrossRef]
5. Zhong, X.; Zhong, W.; Liu, Y.; Yang, C.; Xie, S. Optimal energy management for multi-energy multi-microgrid networks considering carbon emission limitations. *Energy* **2022**, *246*, 123428. [CrossRef]
6. Kong, L.; Shi, L.; Shi, Z.; Wang, S.; Cai, G. Low-carbon optimal dispatch of electric-hydrogen-heat system in park based on alternating direction method of multipliers. *Trans. China Electrotech. Soc.* **2023**, *38*, 2932–2944.
7. Kong, H.; Fu, Y.; Jia, Q.; Zhang, T.; Meng, D. Low carbon optimization of integrated energy microgrid based on life cycle analysis method and multi time scale energy storage. *Renew. Energy* **2023**, *206*, 60–71.
8. Mirzapour-Kamanaj, A.; Majidi, M.; Zare, K.; Kazemzadeh, R. Optimal strategic coordination of distribution networks and interconnected energy hubs: A linear multi-follower bi-level optimization model. *Int. J. Electr. Power Energy Syst.* **2020**, *119*, 105925. [CrossRef]
9. Hua, W.; Jiang, J.; Sun, H.; Wu, J. A blockchain based peer-to-peer trading framework integrating energy and carbon markets. *Appl. Energy* **2020**, *279*, 115539. [CrossRef]
10. Feng, P.; He, X. Mixed neurodynamic optimization for the operation of multiple energy systems considering economic and environmental aspects. *Energy* **2021**, *232*, 120965. [CrossRef]
11. Liu, Y.; Xiao, H.; Liu, X.; Yu, X.; Zhang, Y.; Lv, G.; Li, X. Low-carbon optimal scheduling for hybrid wind/PV/storage microgrids considering GEC trading and carbon emission constraints. *Zhejiang Electr. Power* **2024**, *43*, 66–73.
12. Si, F.; Zhang, N.; Wang, Y.; Kong, P.-Y.; Qiao, W. Distributed Optimization for Integrated Energy Systems with Secure Multiparty Computation. *IEEE Internet Things J.* **2022**, *10*, 7655–7666. [CrossRef]
13. Teng, F.; Ban, Z.; Li, T.; Sun, Q.; Li, Y. A Privacy-Preserving Distributed Economic Dispatch Method for Integrated Port Microgrid and Computing Power Network. *IEEE Trans. Ind. Inf.* **2024**, *20*, 10103–10112. [CrossRef]
14. Hu, J.; Cao, J.; Chen, M.; Yu, J.; Yao, J.; Yang, S.; Yong, T. Load following of multiple heterogeneous TCL aggregators by centralized control. *IEEE Trans. Power Syst.* **2016**, *32*, 3157–3167. [CrossRef]
15. Yu, H.; Zhang, J.; Ma, J.; Chen, C.; Geng, G.; Jiang, Q. Privacy-preserving demand response of aggregated residential load. *Appl. Energy* **2023**, *339*, 121018. [CrossRef]
16. Yu, H.; Xu, C.; Wang, W.; Geng, G.; Jiang Q. Communication-Free Distributed Charging Control for Electric Vehicle Group. *IEEE Trans. Smart Grid* **2023**, *15*, 3028–3039. [CrossRef]
17. Yuan, Z.; Li, P.; Li, Z.; Xia, J. A Fully Distributed Privacy-Preserving Energy Management System for Networked Microgrid Cluster Based on Homomorphic Encryption. *IEEE Trans. Smart Grid* **2023**, *15*, 1735–1748. [CrossRef]
18. Zou, B.; Chen, G.; Zhang, H.; Song, Y. Improved Divergence-based Distributionally Robust Chance-Constrained Scheduling for Geo-distributed Internet Data Centers. *CSEE J. Power Energy Syst.* **2024**, *early access*.
19. Mhanna, S.; Chapman, A.C.; Verbič, G. A fast distributed algorithm for large-scale demand response aggregation. *IEEE Trans. Smart Grid* **2016**, *7*, 2094–2107. [CrossRef]
20. Latifi, M.; Khalili, A.; Rastegarnia, A.; Bazzi, W.M.; Sanei, S. A robust scalable demand-side management based on diffusion-admm strategy for smart grid. *IEEE Internet Things J.* **2020**, *7*, 3363–3377. [CrossRef]